

# Synthesis and Characterization of Magnetite-Pectin-Alginate Hybrid Bionanocomposite

Biswal T<sup>1</sup>, Barik B<sup>1</sup> and Sahoo PK<sup>2</sup>

<sup>1</sup>Department of Chemistry, VSSUT, Burla, Odisha, India

<sup>2</sup>Department of Chemistry, Utkal University, Bhubaneswar, Odisha, India

\*Corresponding author: Biswal T, Department of Chemistry, VSSUT, Burla, Odisha, India 768018, E-mail: tirnath.biswal@gmail.com

**Citation:** Biswal T, Barik B, Sahoo PK (2016) Synthesis and Characterization of Magnetite-Pectin-Alginate Hybrid Bionanocomposite. *J Mater Sci Nanotechnol* 4(2): 203. doi: 10.15744/2348-9812.4.203

**Received Date:** July 23, 2016 **Accepted Date:** October 13, 2016 **Published Date:** October 17, 2016

## Abstract

It is a one pot synthesis of hybrid bionanocomposite comprising of inorganic magnetite with stabiliser biopolymer pectin and alginate in co-precipitation method using sodium hydroxide and ammonium hydroxide as precipitating agents. A lot of comparison and investigation has been done in particle size of nanocomposite by changing the stoichiometric ratio of both magnetite and bio polymer concentration and drying condition of composite. The nanocomposite has been characterized using infrared spectroscopy (FTIR), scanning electron microscopy (SEM), X-ray powder diffraction (XRD) and (UV-analyser). SEM showed particle size of the nanocomposite and FTIR data confirmed the COO-Fe linkage between polymer COOH group and Fe<sub>3</sub>O<sub>4</sub>.

**Keywords:** Nanocomposite; Biopolymer; Pectin; Alginate

## Introduction

The current and growing interest of nanotechnology results a lot of numerous potential application such as material development, biomedical sciences, electronic, optics, magnetism, energy storage and electrochemistry [1-6]. Superparamagnetic nanocomposite is an important class of advanced nanomaterial. Nano sized material display properties that differ from their respective bulk material [7]. Magnetic nanomaterials are one of important and interesting classes because of their current and potential is biological, biomedical and environmental application. Due to low toxicity, biocompatibility, cost-effectiveness and high surface area to volume ratio as function of particle size, when combined with their ability for surface chemical modification, represent major advantages compared to other nanoparticle [3,8-11]. Magnetite and maghemite are two main form of iron oxide nanoparticle with diverse applications. Magnetite nanoparticle size less than 20nm are regarded as superparamagnetic as each particle is composed of a single domain. The successful approaches to the synthesis of magnetic nanoparticle uses capping/ stabilisation agents which may be a simple molecule or polymeric material. Among the polymeric capping agents, biopolymer like pectin, chitosan, alginate, zein and chitin are special interest due to their biocompatibility and biodegradability. Pectin and alginate are complex polysaccharide that contain 1,4- $\alpha$ -D-galacturonic acid [12]. Pectin has a very complex structure that depends on both its source and extraction process. Its properties depend on degree of esterification [13]. Pectin has been used extensively in food, cosmetics, pharmaceutical and biomedical industries for their gel forming properties in the presence of multivalent cations. Pectin is biodegradable, biocompatible, and bioactive [14]. Pectin also contains the hydroxyl group which enhances the chemical properties and COOH group which binds Fe<sub>3</sub>O<sub>4</sub> with coordinate covalent bond.

Co-precipitation and high temperature solution phase methods are two most widely used methods for synthesis of iron oxide nanoparticles. The high temperature solution method involves the decomposition of iron organic precursor Fe(acac)<sub>3</sub>, Fe(CO)<sub>2</sub> etc. So co-precipitation method involves the co-precipitation of ferric and ferrous ions using base such as (NaOH) or (NH<sub>4</sub>OH) in aqueous medium. This method is favourable for the reaction condition at room temperature and using environmental eco-friendly materials.

Generally, in presence of air and moisture iron will oxidise and corrosion occurs. So to save iron we are coating different metals on surface of iron. The same concept was taken here to save magnetite nanoparticle. we had given polysaccharide coating on magnetite nanoparticle. The stabilisation of magnetic nanoparticle by coating them with non-toxic polymeric materials reduces toxicity of magnetite nanoparticle in living system. The use of natural occurring polymers as stabilising or capping agent for magnetite nanoparticle is considered as green chemistry approach [15,16].

In this paper we prepared magnetite polymer of hybrid bionanocomposite with close control over particle size, shape and size distribution by mixing ferric and ferrous chloride with two natural occurring polymer pectin and alginate using NaOH or  $\text{NH}_4\text{OH}$  as precipitating agent with special references [17,18].

## Experimental

### Materials

Ferric chloride ( $\text{FeCl}_3 \cdot 6\text{H}_2\text{O}$ ) of spectrochem, ferrous chloride ( $\text{FeCl}_2 \cdot 4\text{H}_2\text{O}$ ) of spectrochem, sodium hydroxide (NaOH) is of fine chemical ltd, ammonium hydroxide solution ( $\text{NH}_4\text{OH}$ ) of Spectrochem, Pectin 38% esterified of Lobal Chemie and sodium salt of alginate of Lobal Chemie.

### Methods

The solution of Pectin and alginate (1:1) of different concentrations (%W/V) were dissolved in 250 ml of distilled water (Table 1). It was degassed with nitrogen for 30 minutes to deoxygenate the solution. 50 ml solution of ferric and ferrous chloride (2:1 molar ratio) in water was added in the reaction flask. The volume of the reaction mixture was maintained 300 ml and the reaction mixture was again degassed with nitrogen for 20 minutes. Now colour of the solution becomes brown. Then base (1.5 M) was added drop wise using a syringe till the solution become completely black. It indicates the formation of magnetite.

Then it was filtered and the residue was washed several times with distilled water until the pH reduced to 7. Half amount of the black precipitate was dried with air and remaining half was freeze dried and characterized.

Sample	Fe <sup>3+</sup> /Fe <sup>2+</sup>	Weight of Fe <sup>3+</sup> salt(g)	Weight of Fe <sup>2+</sup> salt(g)	[Pectin]. (%w/v)	[alginate] (%w/v)	Precipitating agent
PAIO	2:1	14.4	4	00	00	NH <sub>4</sub> OH
PAIO-1	2:1	7.8	3	0.15	0.15	NH <sub>4</sub> OH
PAIO-2	2:1	7.8	3	0.25	0.25	NaOH
PAIO-3	2:1	7.8	3	0.4	0.4	NH <sub>4</sub> OH

Table 1: Reaction parameters and condition

## Results and Discussion

The effect of the precipitating agent NaOH and  $\text{NH}_4\text{OH}$  in the above experiment was described below in Table 2.

Since NaOH is a base in precipitating agent, the solution has pH of about 13. At this pH, the ester part of polymer hydrolyses to acid form. So the obtained polymer becomes powder form.

The exclusive powder was produced due to depolymerisation of polymer (pectin and alginate) chain by stronger base (NaOH). When  $\text{NH}_4\text{OH}$  solution is used as precipitating agent then gel type product was obtained. It indicates that due to weak base the limiting de-esterification had taken place. So the polymer gel network was obtained.

The difference in pH can be attributed to the difference in the influence of the base on pectin and alginate.  $\text{NH}_4\text{OH}$  will neutralise free carboxylic acid groups in the process of amidation.  $\text{NH}_4\text{OH}$  is however a weak base to cause the amidation of polymer. When we using  $\text{NH}_4\text{OH}$  as precipitating agent, the ester form of both pectin and alginate become amide ( $-\text{CONH}_2$ ). But when NaOH is used as precipitating agent the ester forms of both pectin and alginate became salt of carboxylic acid ( $-\text{COO}^-$ ). Due to strong electronic force of attraction between  $-\text{COO}^-$  and Fe(II) and Fe(III) the composite became powder in nature. But in case of  $\text{NH}_4\text{OH}$  or amidation the force of attraction between  $\text{CONH}_2$  and Fe(II) /Fe (III) is weak coordinate covalent type in nature. Hence the so obtaining nanocomposite became gel type network instead of solid powder.

Sample	Base used as precipitating agent	Nature of product
PAIO-0	$\text{NH}_4\text{OH}$	Powder
PAIO-1	$\text{NH}_4\text{OH}$	Powder plus gel-network
PAIO-2	NaOH	Powder
PAIO-3	$\text{NH}_4\text{OH}$	Gel-network

PAIO → Pectin-alginate iron oxide

Table 2: Effect of the precipitating agent NaOH and  $\text{NH}_4\text{OH}$

### X-Ray Diffraction (XRD) Analysis

Figure 1 shows the XRD patterns of PAIO-2 and PAIO-1 nanocomposites. The diffraction peaks indicating the formation of other compounds are absent. The diffraction patterns have well defined peaks which indicates that the samples are crystalline.

The diffraction peaks are indexed as (220), (311), (400), (422), (440), and (511) crystal planes, corresponding to a cubic unit cell of magnetite, and they match the inverse-spine structure of magnetite (space group of  $Fd\bar{3}m$ , JCPDS Card no.79 - 0417) [15]. The co-precipitation of maghemite is excluded by the absence of the (210) and the (110) peaks, which in the case of maghemite are present and at slightly higher intensities than the (111) peak. The diffraction peaks of PAIO-2 are broader than those of PAIO-1, indicating the finer nature and smaller crystallite sizes of the particles. The average particle sizes were calculated using the Scherrer equation [19]:

$$D_{hkl} = \frac{k\lambda}{b \cos \theta}$$

Where  $D_h$  is the average particle size; the equation uses the corrected reference peak width at angle  $\theta$ .  $\lambda$  is the X-ray Wavelength, is the corrected width of the XRD peak at half height, and  $k$  is the shape factor, which is approximated as 0.9 for magnetite [15]. Interestingly, the particle sizes of PAIO-1A and PAIO-1F, PAIO-2A and PAIO-2F were found to be the same, meaning the drying conditions had no effect on the particle sizes. The calculated values are summarised in Table 2. The inter-plane spacing ( $d_{hkl}$ ) of the (311) diffraction was calculated using the equation [20].

$$d_{hkl} = \frac{\lambda}{2 \sin \theta}$$

The calculated  $d_{hkl}$  values for PAIO-1 and PAIO-2 were found to be 2.533 °Å and 2.528 °Å, respectively. Comparing these values to the standard values for magnetite (2.532 °Å; JCPDS no. 19-629) and maghemite (2.518 °Å; JCPDS no. 39-1346), we can conclude that only magnetite is present in the nanocomposites. The lattice parameters of the (311) diffraction was determined by Bragg's Law [20].

$$d_{hkl} = \frac{a}{\sqrt{h^2 + k^2 + l^2}}$$

They were found to be 8.401 and 8.384 for PAIO-1 and PAIO-2, respectively. The calculated values were found to be closer to the standard value of magnetite (8.391; JCPDS no. 79-0417) than those of maghemite (8.347).

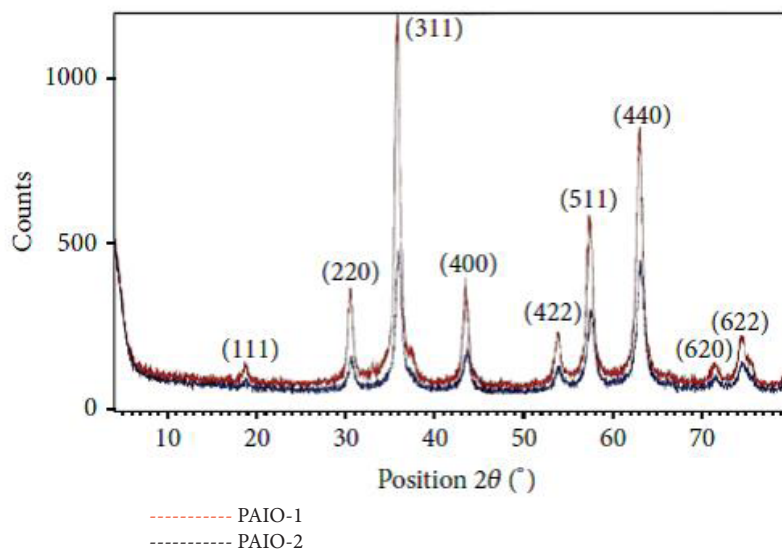


Figure 1: XRD patterns of PAIO-2 and PAIO-1 nanocomposites

### Fourier-Transform Infrared Spectral Characterization (FTIR)

The FTIR spectrum of pure pectin and alginate has a broadband at  $3429 \text{ cm}^{-1}$  and  $3390 \text{ cm}^{-1}$  respectively, which can be attributed to the (O-H) stretching vibration of the hydroxyl group. The intense peak for pectin and alginate at  $1633 \text{ cm}^{-1}$  and  $1634 \text{ cm}^{-1}$  is characteristic of the carbonyl (C=O) stretching vibration of an ester. The bands at  $1680, 1385 \text{ cm}^{-1}$  are characteristic of asymmetric and symmetric stretching of the carboxylate group of alginate and pectin [20]. The band at  $1077 \text{ cm}^{-1}$  and  $1061 \text{ cm}^{-1}$  in both pectin and alginate is assigned to the C-O bending vibration. This band is substantially reduced in intensity in nanocomposites form. Comparing data of Figure 4 with Figure 2 and 3. The FTIR spectra of pectin and the coated magnetite nanocomposites are similar to those reported in the literature [10,20]. Two new peaks  $1586 \text{ cm}^{-1}$ -  $1587 \text{ cm}^{-1}$  and  $1394 \text{ cm}^{-1}$  -  $1376 \text{ cm}^{-1}$  have been attributed to symmetric and asymmetric stretching of carboxylic-metal (COO-Fe) linkage [19-21]. The presence of peaks due to pectin in the

nanocomposites supports the fact that both pectin and alginate actually coats the magnetite. The reduction of intensity at 1017  $\text{cm}^{-1}$  result from breaking of glycosidic bonds, hence de-polymerization of both pectin alginate. While reduction in peak intensity at 1746  $\text{cm}^{-1}$  is as result of significant de-esterification of ester group of pectin polymeric chain. These FT-IR results support the suggestion that NaOH causes significant depolymerisation of biopolymer, while  $\text{NH}_4\text{OH}$  does not.

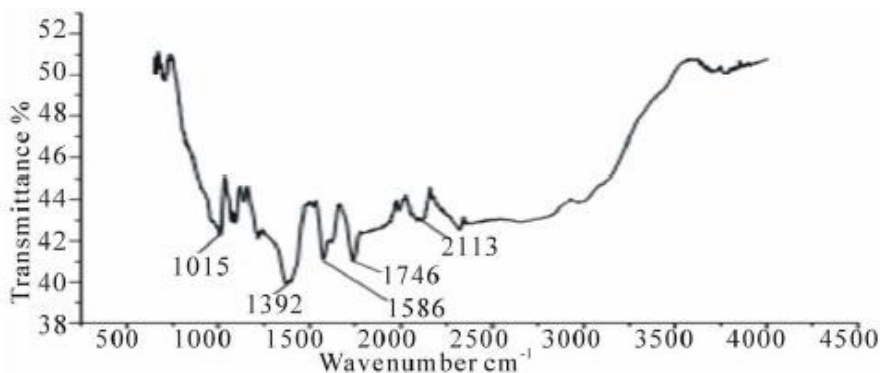


Figure 2: FTIR spectra of PAIO-1

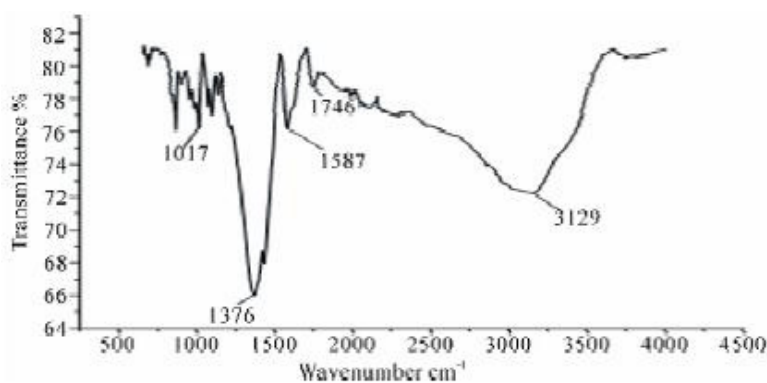


Figure 3: FTIR spectra of PAIO-2

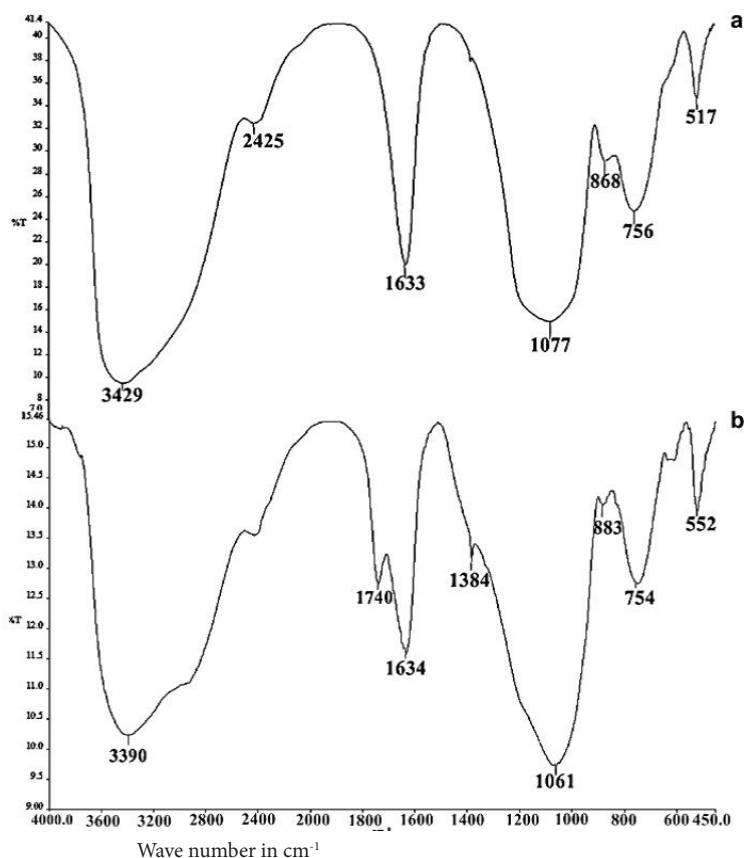


Figure 4: FTIR spectra of both (a-pectin) and (b-alginate)

## Electron Microscopy

The estimated mean particle diameter measured from the TEM images is found to be consistent with the XRD results (Table 3). The effect of the drying method on the nanocomposite can be seen in the TEM images, where the air-dried samples exhibited some shrinkage, observed as tearing of films (Figure 7 and 8). Figures 5 and 6 shows more uniformity of pore size, shape and distribution, suggesting less or more uniform shrinkage of the nanocomposite during freeze-drying, while many of the particles are coated in pectin and alginate, nanoparticles were also clearly found on the surface of both PAIO-1A and PAIO-1F. This outcome is attributed to the high magnetite to both pectin and alginate ratio, especially in PAIO-1A and PAIO-1F.

Sample	Average particle size (nm) from PXRD	Particle size distribution (nm) from TEM
PAIO-1	13	5-18
PAIO-2	9	7-13

**Table 3:** Estimated particle size and particle size distribution

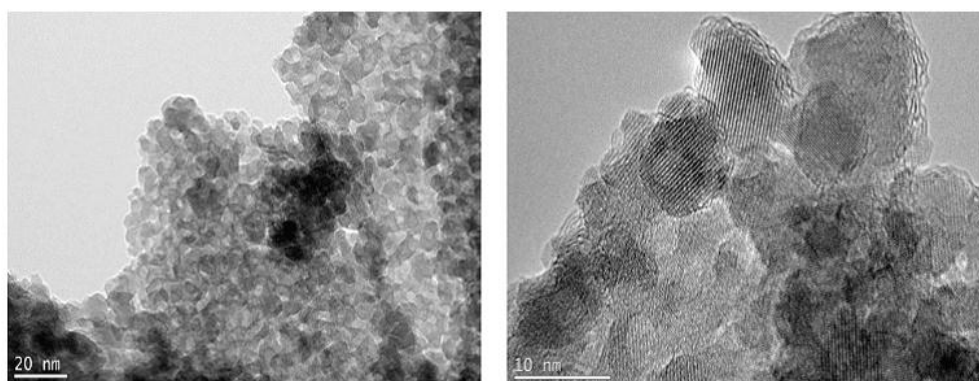


**Figure 5:** TEM image of PAIO-2F

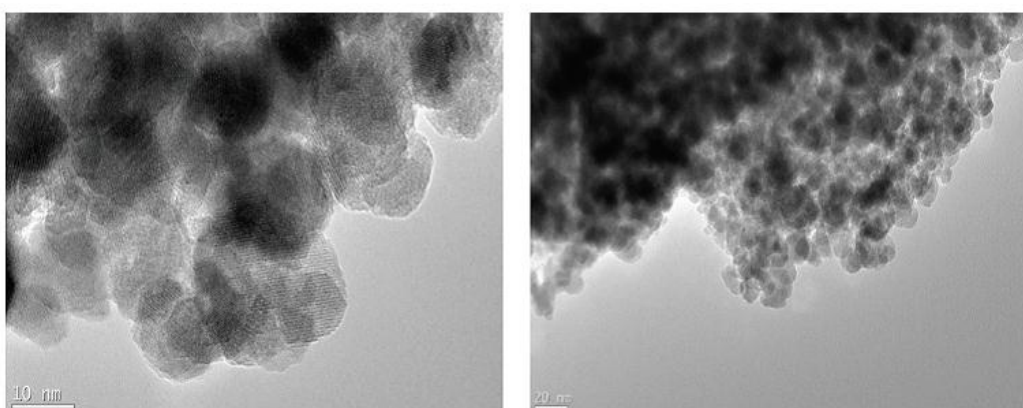


**Figure 6:** TEM image of PAIO-1F

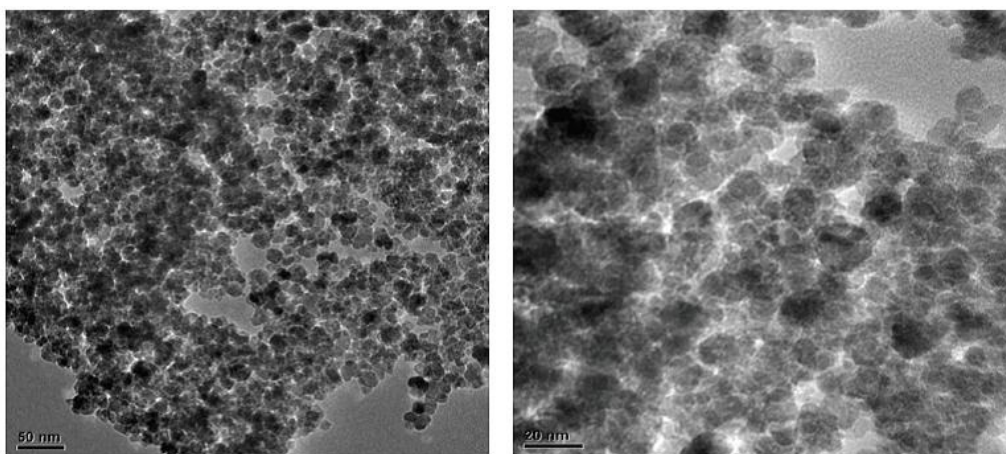
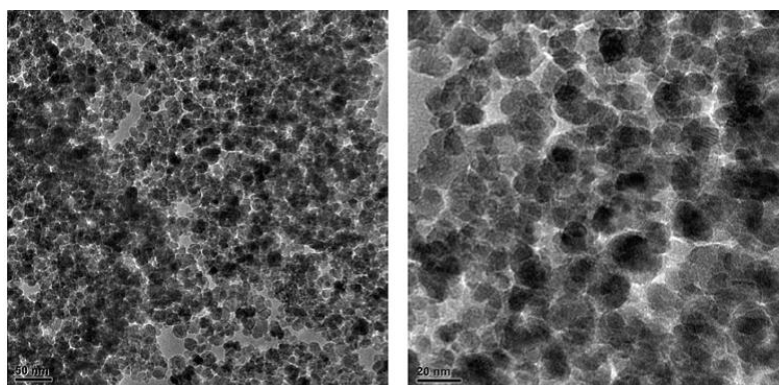


**Figure 7:** TEM image of PAIO-2A



[PAIO-A (pectin alginate iron oxide air dried)]  
 [PAIO-F (pectin alginate iron oxide freeze dried)]  
**Figure 8:** TEM images of PAIO-1A

## Magnetic Properties

The magnetic properties of nanoparticles are highly dependent on the particle size. In order to have superparamagnetic nanoparticles the nanoparticles must have a mean diameter of less than 20 nm. For superparamagnetic nanoparticles to have a high saturation magnetization, the agglomeration of these particles after synthesis must be overcome. Figures 9, 10, 11 and 12 show the magnetic susceptibility of the nanocomposites at a constant temperature of 300K under varying magnetic fields. Table 3 shows estimated particle size and particle size distribution of the nanocomposite. It was observed that the samples rise to maximum magnetisation very rapidly, and this observation is similar to that of super paramagnetic nanocomposites at room temperature reported in the literature [20,21]. This indicates that the particles can be controlled by an external magnetic field. The inter particle distance is an important factor that affects the saturation magnetization values of magnetic nanoparticles as the strength of the magnetic moment interaction depends on the inter particle distance [10]. This is evident in the results presented in Table 3, as both PAIO-1F and PAIO-2F have the highest saturation magnetization values of 53 and 54 emu/g, respectively, in spite of the difference in the magnetite to pectin ratios. This can be attributed to the fact that, during the freeze-drying process, there was less shrinkage in the polymer cage hosting the nanoparticles than in the case with the air-dried particles [22,23]. The air-dried nanocomposites shows a drop in the saturation magnetization values, this is due to the shrinkage of the polymer host during drying, reducing the inter particle distance. These results in an increased interparticle magnetic moment interaction and a consequent decrease in the total magnetization [24,25]. Comparing the saturation magnetization values of PAIO-1A and PAIO-1F, the net difference is 22 emu/g which is greater than the difference of 8 emu/g, for PAIO-2A and PAIO-2F [26,27]. This outcome shows that the saturation magnetization does not only depend on the drying conditions but also on the reactant ratios, as PAIO-1 nanocomposites have a higher magnetite to pectin ratio compared to the PAIO-2 nanocomposite. It was seen that the magnetisation values with pectin coating are higher than the values found in the literature for air-dried samples. There is a significant drop in magnetisation values of the air dried nanocomposites, compared to that of pure magnetite nanoparticle. This is due to the formation of magnetic dead layer by pectin at the domain boundary wall of MNPs [20]. This drop in magnetisation is not observed in our work, especially for the freeze-dried samples. Further work on the application of these nanoparticles to the treatment of disease is on-going, but early results using simple turbidity measurements in water medium shows that these nanocomposites do not agglomerate indicating the suitability of this polymer coating for biomedical applications. Gels may also be used for producing free-standing films and coatings, opening up the possibility of fabricating more robust components.

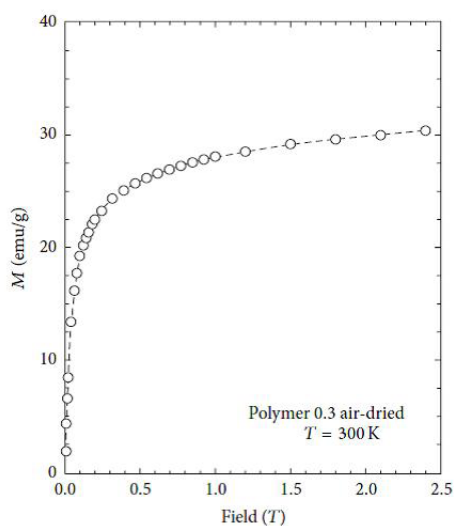


**Figure 9:** Magnetization curve of PAIO-1A at 25 °C

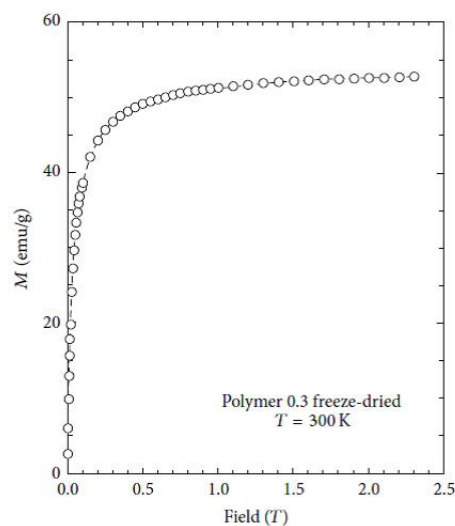


**Figure 10:** Magnetization curve of PAIO-1F at 25 °C

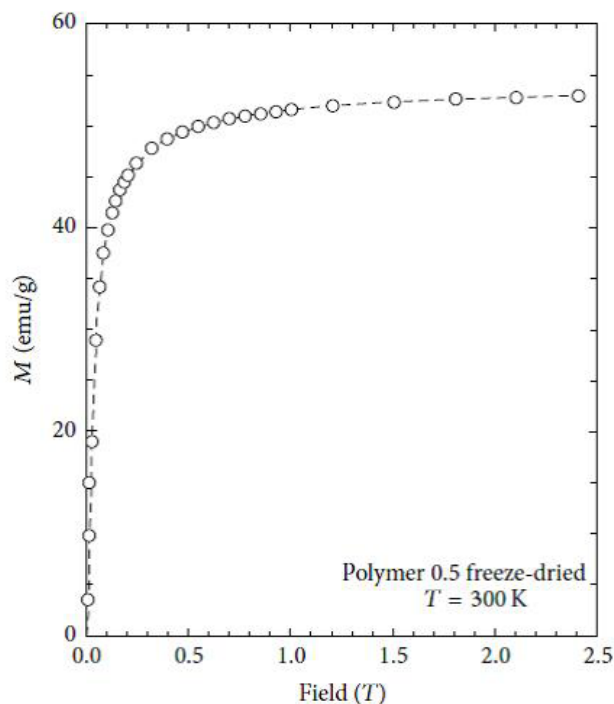


Figure 11: Magnetization curve of PAIO-2F measured at 300K

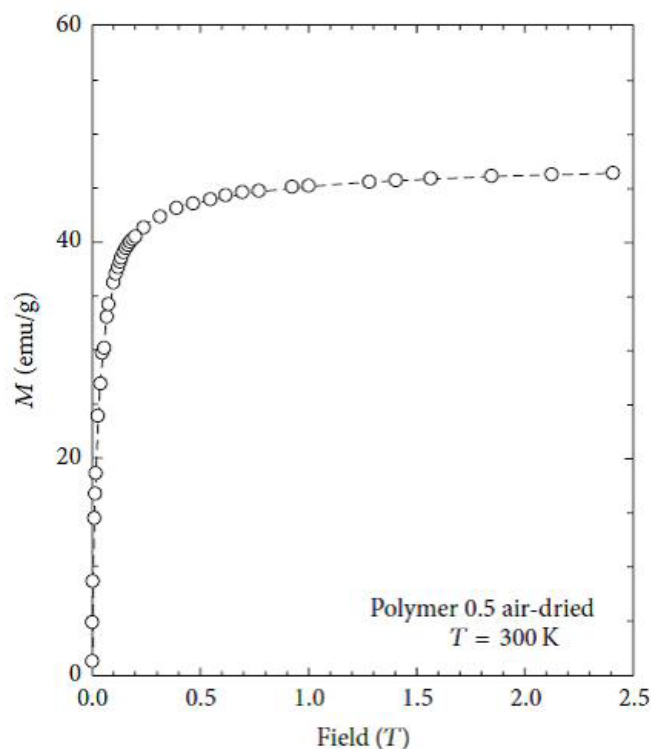


Figure 12: Magnetization curve of PAIO-2A measured at 300K

## Conclusion

We report the synthesis of nanocomposites of superparamagnetic magnetite nanoparticles in a pectin matrix with high saturation magnetization of 53 emu/g and 54 emu/g and demonstrated the dependence of the magnetic properties of these nanocomposites on the drying conditions and reactant ratios. The particle size and homogeneity were controlled by the presence of the pectin. Thus a facile in situ co-precipitation synthetic approach of magnetite-pectin nanocomposite at room temperature has been demonstrated. Freeze-drying is routinely used for the production of fruits, vegetables, and pharmaceutical products. The combination of the facile precipitation method and freeze-drying presents the possibility for producing large quantities of SPION-based composites with better control over properties and particle size. Such nanocomposites have promising biomedical and environmental applications and supports green chemistry.

## References

1. Pankhurst QA, Connolly J, Jones SK, Dobson J (2003) Application of Magnetic Nanoparticles in Biomedicine. *J Phys D: Appl Phys* 36: 167-81.
2. Niemeyer CM (2001) Nanoparticle, proteins and Nucleic acids Biotechnology Meets Material Science. *Angewandte ChemIE Int Ed* 40: 4128-58.
3. Jana D, Radim H, Vojtech A, Rene K, Oidrich S, et al. (2009) Preparation and properties of Various Magnetic Nanoparticle. *Sensors* 9: 2352-62.
4. Lodhia J, Mondarano G, Ferris NJ, Eu P, Cowell SF (2010) Development and Use of iron Oxide Nanoparticle. *Biomed Imaging Interv J* 6: e12.
5. Zhang L, He R, Gu H-C (2006) Synthesis and kinetic Shape and Size Evolution of magnetic Nanoparticle. *Mater Res Bullet* 41: 260-7.
6. Henedez R, Sacristán J, Nogales A, Ezquerro TA, Mijangos C (2009) Structural Organization of Iron Oxide Nanoparticles Synthesized Inside Hybrid Polymer Gels Derived from Alginate Studied with Small-Angle X-ray Scattering. *Langmuir* 25: 13212-8.
7. Gubin SP, Spichkin YI, Yurkov GY, Tishin AM (2002) Nanomaterial for High-Density Magnetic Data Storage. *Russian J Inorganic Chem* 47: S32-67.
8. Crini G (2006) Non-conventional Low-cost Adsorbents for Dye Removal: A Review. *Biosour Technol* 97: 1061-85.
9. Dalali N, Khoramzad M, Habibzadeh M, Faraji M (2011) Magnetic Removal of Acidic Dyes from waste water Using Surfactant-Coated Magnetic Nanoparticles: Optimisation of Process by Taguchi Method. *IPCBE* 15: 89-93.
10. Gong JL, Wang XY, Zeng GM, Chen L, Deng JH, et al. (2012) Copper(II) Removal by pectin-Iron oxide Magnetic Nanocomposite Adsorbent. *Chem Engineer J* 185-86: 100-7.
11. Daniel-da-Silva AL, Trindade T, Goodfellow BJ, Costa BFO, Correia RN, et al. (2007) In situ Synthesis of Magnetite Nanoparticle in Carrageenan Gels. *Bio-macromolecules* 8: 2350-7.
12. Mollea C, Cheampo F, Conti R (2008) Extraction and Characterization of Pectin from Cocoa Husks: A preliminary study. *Food Chem* 107: 1353-6.
13. Racoviță S, Vasiliu S, Popa M, Luca C (2009) Polysaccharides Based on Micro and Nanoparticle Obtained by Ionic gelation and Their Application as Drug delivery System. *Revue Roumaine de Chemie* 54: 709-18.
14. Sharma BR, Naresh L, Dhuldhoya NC, Merchant SU, Merchant UC (2006) An overview on pectin. *Times Food Process J* 23: 44-51.
15. Kushwaha OS, Ver Avadhani C, Tomer NS, Singh RP (2014) Accelerated Degradation Study of Highly Resistant Polymer Membranes for Energy and Environment Applications. *Adv Chem Sci* 3: 19-30.
16. Kushwaha OS, Avadhani CV, Singh RP (2013) Photo-oxidative degradation of polybenzimidazole derivative membrane. *Adv Mater Lett* 4: 762-8.
17. Lonkar SP, Kushwaha OS, Leuteritz A, Heinrich G, Singh RP (2012) Self photostabilizing UV-durable MWCNT/polymer nanocomposites. *RSC Adv* 2: 12255-62.
18. Kushwaha OS, Avadhani CV, Singh RP (2015) Preparation and characterization of self-photostabilizing UV-durable bionanocomposite membranes for outdoor applications. *Carbohydr Polym* 123: 164-73.
19. Iida H, Takayanagi K, Nakanishi T, Osaka T (2007) Synthesis of Fe<sub>3</sub>O<sub>4</sub> nanoparticles with various sizes and magnetic properties by controlled hydrolysis. *J Colloid Interface Sci* 314: 274-80.
20. Dai J, Wu S, Jiang W, Li P, Chen X, et al. (2013) Facile Synthesis of Pectin Coated Fe<sub>3</sub>O<sub>4</sub> Nanospheres by the Sonochemical Method. *J Magnetism Magnetic Mater* 331: 62-6.
21. Predoi D, Andronescu E, Radu M, Munteanu MC, Dinischiotu A (2010) Synthesis and Characterization of Bio-Compatible Maghemite Nanoparticles. *Digest J Nanomater Biostructur* 5: 779-86.
22. Guo L, Liu G, Hong RY, Li HZ (2010) Preparation and Characterization of chitosan poly (acrylic acid) magnetic microspheres. *Marine Drugs* 8: 2212-22.
23. Wilson KS, Harris LA, Goff JD, Riffle JS, Dailey JP (2002) A generalized method for magnetite nanoparticle steric stabilization utilizing block copolymers containing carboxylic acids. *European Cells Mater* 3: 206-9.
24. El Ghandour H, Zidan HM, Khalil MMH, Ismail MIM (2012) Synthesis and some physical properties of magnetite(Fe<sub>3</sub>O<sub>4</sub>) nanoparticles. *Int J of Electrochem Sci* 7: 5734-45.
25. Zhang L, He R, Gu HC (2006) Oleic acid coating on the monodisperse magnetite nanoparticles. *Appl Surface Sci* 253: 2611-7.
26. Mamani JB, Costa-Filho AJ, Cornejo DR, Vieira ED, Gamarra LF (2013) Synthesis and characterization of magnetite nanoparticles coated with lauric acid. *Mater Character* 81: 28-36.
27. Ruiz-Moreno RG, Martinez AI, Castro-Rodriguez R, Bartolo P (2013) Synthesis and characterization of citrate coated magnetite nanoparticles. *J Superconduct Novel Magnet* 26: 709-12.

Submit your next manuscript to Annex Publishers and benefit from:

- ▶ Easy online submission process
- ▶ Rapid peer review process
- ▶ Online article availability soon after acceptance for Publication
- ▶ Open access: articles available free online
- ▶ More accessibility of the articles to the readers/researchers within the field
- ▶ Better discount on subsequent article submission

Submit your manuscript at

<http://www.annexpublishers.com/paper-submission.php>